Escape dynamics of coupled particles in nonlinear, disordered lattices

K. Manski

Institut für Physik, Humboldt-Universität zu Berlin, Newtonstrasse 15, 12489 Berlin, Germany

D. Hennig

Department of Mathematics, University of Portsmouth, Lion Gate Building, Lion Terrace, Portsmouth PO1 3HF, United Kingdom
(Received 22 June 2009; published 10 November 2009)

We consider the deterministic escape dynamics of a lattice chain of harmonically coupled particles from a metastable state over a one-dimensional potential barrier. While the case of periodic lattices has already been elaborated, the aim of the present work is to explore the extension to nonperiodic, i.e., disordered, lattices. Each particle evolves in an individual local potential, which is characterized by a harmonic term and a nonlinear term. Two kinds of parametric disorder are considered. "Disorder in nonlinearity" is only caused by different nonlinear terms—"disorder in harmonicity" only by different harmonic terms. We assure that the two kinds of disorder, with their individual potential barriers uniformly distributed around a globally equal mean barrier height, exhibit a comparable strength of disorder. Starting with an initial completely delocalized state, we observe localization of energy and formation of breathers ensues. It is shown that increasing disorder in nonlinearity decreases the mean escape time opposite to increasing mean escape times resulting from increased disorder in harmonicity. Comparison with the mean escape time obtained for a third kind of parametric disorder characterized by overall equal barrier heights leads to the conclusion that indeed inhomogeneous barriers facilitate the speedy escape.

I. INTRODUCTION

Escapes from metastable states and transitions between them play an important role in many physical systems [1,2]. An energetic barrier blocks the escape from the metastable state to an adjacent attracting domain. One means of overcoming the barrier is due to the injection of sufficiently enough energy into the system supplied by an external heat bath. On the other hand, in the absence of any external energy source, the energy once allocated has to suffice for performing the task of barrier crossing. In such microcanonical situations, solely the underlying deterministic and conservative nonlinear dynamics promotes escape events as described in [3]. There, it has been demonstrated that the barrier crossing of a chain of coupled nonlinear oscillators can be reached spontaneously. In fact, starting with a flat state configuration of the chain, where each of its constituents possesses too little energy to overcome the barrier on its own, the associated critical localized mode, viz., the transition state, can be reached by localizing energy to a few oscillators in a self-organized manner. This nonlinear process, intrinsic to many nonlinear and spatially periodic lattice systems [4,5], is connected with the emergence and enhancement of breather states. Conversely, localization in linear but spatially nonperiodic (disordered) lattice systems is related to the phenomenon of Anderson localization for which all eigenmodes of an one-dimensional system are exponentially localized representing pinned (immobile) states. Hence, no energy transport is possible.

The interplay between nonlinearity and disorder with regard to energy transport in disordered nonlinear lattice systems has attracted considerable interest lately [4,6–12]. These studies focused interest on the transport properties of systems exhibiting linear Anderson localization when nonlinearity is added. That is, the initial lattice configuration is a localized wave packet. It has been found that with the additional presence of nonlinearity the spreading of an initially localized wave packet is induced [11].

With the present paper, our consideration of the interplay between nonlinearity and disorder is based on an approach opposite to that in [6–12], namely, we consider the possible localization of an initially extended homogeneous lattice state. In more detail, we are interested in self-organized escape dynamics of particles starting from a completely delocalized state in a conservative, deterministic Klein-Gordon lattice with a disordered archetypical anharmonic local potential. The potential exhibits a barrier separating a metastable state from an attractive region. We explore the dynamics of macroscopic discrete, nonlinear oscillator chains in such a metastable potential. This may appear as a realistic model for molecular chains which exit out of basins of attraction or surmounting energetic thresholds. Furthermore, it may describe the breaking of bound states of duplex chains or a molecular chain crossing a spatial barrier that blocks the immediate access to a reactant pathway. The ordered limiting case of our system has been studied in [3,13–16]. For long chains, a formation of discrete breathers occurs from an almost homogeneous initial state due to modulational instability. As a result, a successive escape of the particles beyond the barrier is caused providing the associated transition state is overcome. Assuming also a constant energy, the question addressed here is: how does disorder of the local potential affect the localization behavior of the system, the escape dynamics, and mainly the escape times? To tackle this problem, a system with displaceable different kinds of disorder and associated adjustable strengths of disorder will be constructed in Sec. II. Due to two independent parameters of the local potential, we treat kinds of disorder that could cause qualitatively different interplay of Anderson localization and discrete breathers and could entail scenarios manifesting

clearly the influence of the nonlinearity or inhomogeneity of the barrier energies on the escape dynamics. The mean escape time of ensembles of systems with various kinds of disorder is calculated in Sec. III A. We show details of the energy localization by consulting measurements which describe the capability of the chain to perform a self-organized escape. In the last part, we concentrate on the important role of the affection of energy localization to certain particles depending on the features of the respective local potential. In the closing, Sec. VI, we formulate a summary and an outlook.

II. DISORDERED, NONLINEAR LATTICE MODEL

We present the disordered, nonlinear lattice model describing the coupled dynamics of N particles constituting a one-dimensional chain. The particles are assumed to be of mass equal one. The conservative and deterministic dynamics is based on the following Hamiltonian:

$$H = \sum_{n=1}^{N} \left[\frac{p_n^2}{2} + U_n(q_n) + \frac{\kappa}{2}(q_{n+1} - q_n)^2 \right] = \text{const} = E. \quad (1)$$

q_n and p_n correspond to the coordinate and momentum of the nth particle, respectively. In addition to motion in the individual potential U_n each particle is harmonically coupled to its nearest neighbors with interaction strength κ. We impose periodic boundary conditions: $q_1 = q_{N+1}$ and $q_N = q_0$.

A. On-site potentials

Disorder is contained in the parameters of the local potential. By disorder, we mean that each oscillator evolves in an individual cubic single well on-site potential of the form

$$U_n(q_n) = \frac{\omega_n^2}{2}q_n^2 - \frac{a_n}{3}q_n^3, \quad \text{with} \quad \omega_n^2 > 0 \quad \text{and} \quad a_n \neq 0,$$

$$(2)$$

whose individuality is characterized by the harmonicity parameter ω_n^2 and the anharmonicity parameter a_n. For fixed values of $\omega_n^2 = 2$, $a_n = 1$ the potential is plotted in Fig. 1. U_n exhibits an equilibrium at $q_{n;\min} = 0$, corresponding to $U_n(q_{n;\min}) = 0$, which is stable for $a_n = 0$ and metastable for $a_n \neq 0$. In case $a_n \neq 0$, a second zero-point of the potential, $U_n = 0$, can be found at

$$q_{n;\text{zero}} = \frac{3\omega_n^2}{2a_n}, \quad (3)$$

and there is, furthermore, a local maximum of the potential at

$$q_{n;\max} = \frac{\omega_n^2}{a_n} \quad (4)$$

representing an energy barrier

$$B_n := U_n(q_{n;\max}) - \underbrace{U_n(q_{n;\min})}_{=0} = \frac{\omega_n^6}{6a_n^2} \quad (5)$$
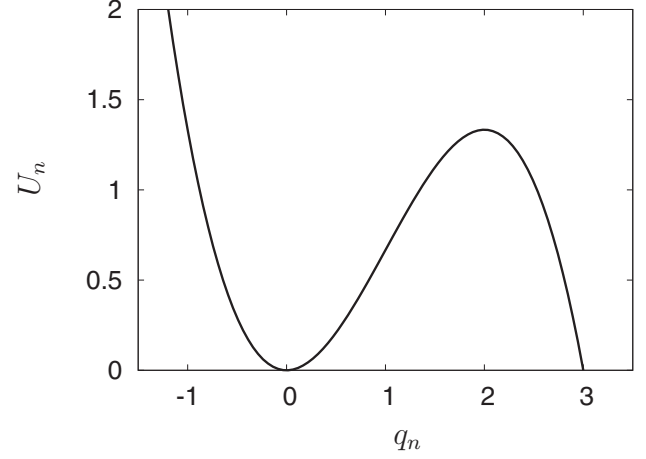
FIG. 1. On-site potential $U_n(q_n)$ given in Eq. (2) with $\omega_n^2 = 2$ and $a_n = 1$.

for particles leaving the well in the positive (negative) direction for $a_n > 0$ ($a_n < 0$). We focus on two main kinds of disorder, which are both connected with inhomogeneous barriers. In addition, we investigate very selectively disorders with homogeneous barriers or without any barriers.

Expecting that the height of the barrier affects the arduousness for the chain to escape from the metastable state, we appoint mean barrier energies.

We consider a chain with $N \gg 1$ particles. The system is deterministic and we understand "disorder" as a stochastic term, i.e., we take a uniform randomized sequence $B_1, B_2, \ldots, B_N$, so that $B_n \in [B - \Delta B, B + \Delta B]$. In these ways, larger values of the "disorder parameter" ΔB express stronger degree of disorder. As shown in [3] for ordered media, the mean escape time the chain needs to overcome the barrier, increases with decreasing ratio of the initial energy to the (homogeneous) barrier energy. Since we are interested in what way different kinds of disorder impede or facilitate the escape and B_n depends on a_n and ω_n^2, we keep the mean barrier of the on-site potentials constant and fix the value $B = 4/3$ throughout the paper.

We distinguish between the following different kinds of disorder.

1. Disorder in a_n

The inhomogeneity in U_n is here caused only by the variable a_n. The site harmonicity parameters are chosen constant

$$\omega_n^2 \overset{!}{=} 2 =: \omega^2, \quad (6)$$

$$\overset{(5)}{\Rightarrow} a_n = \frac{2}{\sqrt{3B_n}}. \quad (7)$$

Concerning the degree of disorder, we assume a maximal value $\Delta B = 0.5$, which allows us to perform simulations in an interval of sufficiently strong degree of disorder that, on the other hand, is not too broad to request unreasonable numerical efforts.

As the influence of different anharmonicity parameter values on the shape of the potential U_n is concerned, we remark

that varying a_n has much weaker effect on the linear regime (near $q_{n;\text{min}}=0$) than on the barrier energies. The larger a_n the lower are the barriers and the closer they are situated to the valley and vice versa.

2. Disorder in ω_n^2

In this case, a_n is constant and ω_n^2 is variable

$$a_n \overset{!}{=} 1 =: a, \tag{8}$$

$$\overset{(5)}{\Rightarrow} \omega_n^2 = \sqrt[3]{6B_n}. \tag{9}$$

ω_n^2 over B_n has a positive slope, but the dependence around $B_n=B$ is nearly linearlike for disorder in a_n.

For lower values of the harmonicity parameter particles have to overcome lower barriers. The influence of disorder in ω_n^2 on the "harmonic" area around $q_{n;\text{min}}=0$ is much stronger than in case of disorder in a_n due to the cubic factor q_n^3, which is multiplied by a_n in the on-site potential expression (2).

The question surrounding the following sections is how these two kinds of disorder influence the escape dynamics from the potential well beyond the barrier. Both kinds show in part remarkable similar features. First, lower barriers come nearer to the potential well. Second, on-site potentials with lower barriers are softer compared to those with higher barriers.

To understand the effect of inhomogeneous barrier heights and the role of the nonlinearity in the cases disorder in a_n and disorder in ω_n^2, we consider separately a disordered scenario with homogeneous barrier height and a linear one with disorder, respectively.

3. Disorder with constant B_n

Apparently, this is not realizable keeping the anharmonicity parameter or the harmonicity parameter constant. We use the sequences a_n from case disorder in a_n given in Eq. (7) to calculate ω_n^2. Arranging

$$\omega_n^2 = \sqrt[3]{6Ba_n^2} \tag{10}$$

yields

$$B_n \overset{(5)}{=} \frac{(\omega_n^2)^3 \overset{(10)}{}}{6a_n^2} = B. \tag{11}$$

Since the sequence a_n has originated from the barrier energies of the case disorder in a_n, i.e., not from the barriers defined through Eq. (11), we have to introduce a special parameter

$$\widetilde{B}_n = \frac{(\omega^2)^3 \overset{(6)}{}}{6a_n^2} = \frac{8}{6a_n^2}, \tag{}$$

which we call the "descriptive parameter." Thus,

$$a_n = \frac{2}{\sqrt{3\widetilde{B}_n}} \tag{12}$$

is the argument to be inserted into Eq. (10) and $\widetilde{B}_n$ are the quantities, which define all on-site potentials of the disorder

with constant B_n and for which the mean value is B. Thus, the (uniform) distribution of $\widetilde{B}_n$ quantifies this disorder, i.e., $\widetilde{B}_n \in [B-\Delta B, B+\Delta B]$.

Regarding once more the definition of U_n in Eq. (2), due to the different powers of the q_n terms the influence of inhomogeneous ω_n^2 on U_n is the more dominant compared to the effect of variable a_n the smaller the values $|q_n|$ are. Thus, disorder with constant barriers resembles for small $|q_n|$ the situation with disorder in ω_n^2 rather than disorder in a_n.

4. Linear disorder

Here, we take ω_n^2 from disorder in ω_n^2 and set $a_n=0$. Hence, the barrier ceases to exist. The values of the descriptive parameter are the barriers from the case disorder in ω_n^2

$$\widetilde{B}_n = \frac{(\omega_n^2)^3 \overset{(8)}{}}{6a^2} \frac{(\omega_n^2)^3}{6}. \tag{}$$

Thus, ω_n^2 yields

$$\omega_n^2 = \sqrt[3]{6\widetilde{B}_n}. \tag{13}$$

Since $a_n=0$, purely harmonic oscillators with variable frequencies remain. The system becomes linear and integrable. The influence of disorder on the region near $q_n=0$ is comparable to the case disorder in ω_n^2 (with $a_n=1$), i.e., it is rather strong.

Regarding the organizations of the different kinds of disorder, we note that first, settling a sequence of the descriptive parameter and second, choose one of the four described cases also determines the sequences a_n, ω_n^2, and thus U_n.

B. Equations of motion

The $2N$ Hamiltonian equations $\partial H / \partial p_n = \dot{q}_n$ and $\partial H / \partial q_n = -\dot{p}_n$ can be written as a system of N equations of second order

$$\ddot{q}_n + \omega_n^2 q_n - a_n q_n^2 - \kappa(q_{n+1} + q_{n-1} - 2q_n) = 0, \quad n=1,\dots,N. \tag{14}$$

We arrange initial conditions of the form

$$q_n(t=0) = 0; \quad p_n(t=0) =: p_0. \tag{15}$$

Therefore, the energy $E=Np_0^2/2$ is initially completely kinetic and does not depend on the disorder contained in the potential term. On the other hand, the chain needs disorder to elongate, i.e., otherwise the problem becomes trivial in terms of equal amplitudes $q_1(t)=q_2(t)=\dots=q_N(t)$ for all times. Furthermore, due to the initial conditions (15) the system energy is at the beginning totally nonlocalized, i.e., every unit has the same energy at $t=0$. So, three questions arise that are physically connected with view to different kinds of disorder.

(a) How fast does the chain localize the energy on their particles?

(b) Is there a maximum permissible degree of localization?

(c) When does an escape over the barrier happen?

For the last question, the statistical research requires a numerically practical specification of the escape event. Likewise, for the study of the ordered limiting case of our system studied in [3], we define an escape time $T_{esc}^{(n)}$ of one unit as the moment, at which it passes through the value $q_{esc} = 5q_{n;max}|_{a_n=1,\omega_n^2=2} = 10$ beyond the barrier. With this value of q_{esc}, it is assured that all values $U_n(q_{esc})$, which are attained in the disordered system, are sufficiently lowered, so that the return of an escaped unit over the barrier into the potential well is practically excluded. Then the escape time T_{esc} of the chain is the average of $T_{esc}^{(n)}$ over all its units.

The numerical integration of the equations of motion was performed using a fourth-order Runge Kutta method. Finally, we remark that the results of our simulations do not depend on a specific choice of initial conditions like the one described above where all the energy is initially of kinetic type. Equivalent results are obtained for initial conditions where in the beginning the kinetic energy is zero and the particles possess only potential energy or the initial energy is a sum of kinetic and potential energy. The key measure in all these cases is the energy content per particle which has amount to only a small part of the barrier energy.

III. ESCAPE DYNAMICS

In this section, we study the dynamics of chains consisting of $N=100$ coupled particles. We deal with different kinds and strengths of disorder in the on-site potentials, while we propose a fixed coupling strength $\kappa=0.3$ and initial values $p_n(t=0) \simeq 0.547$, $q_n(t=0)=0$ according to a homogeneously excited chain at $t=0$.

Thus, without parametric disorder, the excitation of the chain, i.e., the energy distribution, would remain homogeneous for all times due to the defined initial conditions. For a study of the influence of the degree of disorder, we tune the disorder parameter ΔB, enabling us to render the system exiguously disordered or nearly spatially periodic. Yet, one could also take the opposite approach: what is the influence of nonlinearity on phenomena that occur typically in linear nonperiodic (disordered) lattices?

In particular, the impact of disorder on the mobility of discrete breathers occurring in ordered discrete systems is of importance for the escape process. In the latter system, one finds scenarios where breathers collide, forming a new breather with larger amplitude. Ultimately, the mobility could be important in our system to reach strong energy localization (at least) in a region of the lattice enabling passage through the transition state so that the chain can surmount the barrier [3]. If, in general, all breathers are static and have insufficient energy for passing, an escape gets potentially out of reach.

Thus, an imaginable negative influence of disorder on the breather mobility is expected to critically impede the escape dynamics—as a result causing longer escape times. Furthermore, if we suppose alternatively that disorder has no significant effect on the breather mobility, then it would be conceivable that breathers move through the lattice search and focus a sufficiently low barrier $B_n < B$—triggering a dynamical transition of the chain beyond the barrier. It is remarkable

that escapes promoted in this way would occur without the demand for more energy localization compared to the ordered case.

On the other hand, linear waves can become localized in disordered systems due to Anderson localization [17–19]. Then, energy transport properties are degraded [18]. In purely linear disordered systems, Anderson modes are immobile [20]. The disorders included in the model systems considered in [6–12] have their influence on the respective linearized system in common. In contrast, our system with disorder in the nonlinearity parameter a_n and constant ω_n^2 possesses a spatially periodic linearized system and thus plane wave solutions.

A. Influence of disorder on the escape times

In the event of escape, the passing over the barrier does not occur isochronously due to the underlying self-organized chaotic dynamics. Normally, one escaping particle pulls its nearest neighbors and in this manner the chain moves successively beyond the barrier. Meanwhile, the first escaping particle accelerates strongly in the positive direction, whereby a numerical overflow impends. Hence, we restrict the coordinates to the limit $q_{end}=10^4$.

In contrast to the ensemble average of one system over random initial conditions considered in [3] for the ordered limiting case, our mean value for the escape time is obtained by averaging over randomized systems with respective equal initial conditions $q_n(t=0)=0$ and $p_n(t=0) \simeq 0.547$. Hence, every particle has an initial energy $p_n^2(0)/2=0.15$ amounting to 11.25% of the mean barrier height $B=4/3$. In Fig. 2, we show the resulting mean escape times for different strengths of disorder. Interestingly, disorder in a_n (left panel of Fig. 2) facilitates and disorder in ω_n^2 impedes the escape, respectively. For $\Delta B=0.15$ (disorder in a_n), escapes occur on average three times faster than in case of disorder in ω_n^2—for $\Delta B=0.4$, about ten times faster. Declaring this as a main result, in the following, we gather additional information, which illuminate the different influence of disorder on the escape dynamics from various angles.

Let us first have a view on two exemplary spatiotemporal evolutions of the particle energies

$$E_n(t) = \frac{p_n^2}{2} + \frac{\omega_n^2}{2}q_n^2 - \frac{a_n}{3}q_n^3 + \frac{\kappa}{4}(q_{n+1}-q_n)^2 + \frac{\kappa}{4}(q_n-q_{n-1})^2.$$

(16)

We use density plots in Fig. 3 to depict for both kinds of disorder the evolution until the first particle has escaped. The translation between gray scale and energy value is given in the key. The ordinate displays the time and the x axis marks the particle number n. The parameters are the same as in Fig. 2, but the disorder parameter is fixed: $\Delta B=0.4$. In addition, we show the uniformly randomized barrier energy of each particle above the panels of the evolutions. In the system with disorder in a_n (left panel), the particle $n=19$ is the first passing the barrier after approximately 780 time units. For disorder in ω_n^2, the escape occurs expectedly slower. After approximately 3600 time units, the particle $n=60$ passes be-
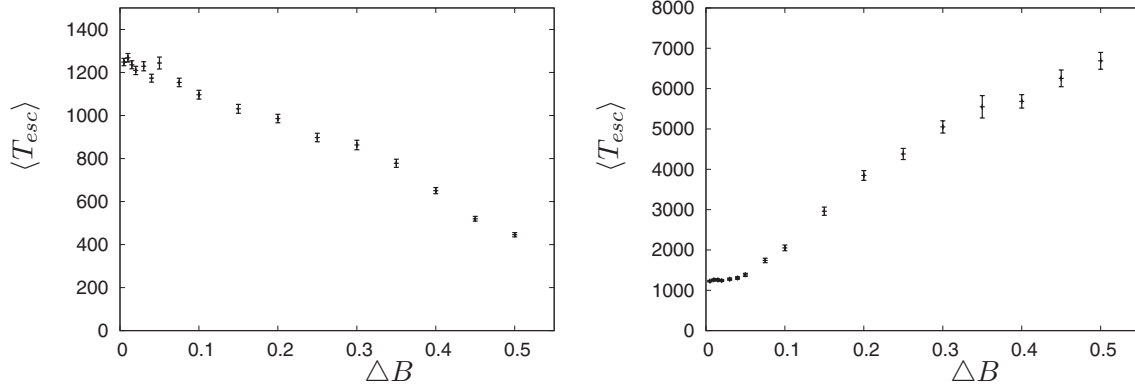
FIG. 2. Mean escape times $\langle T_{esc} \rangle$ for disorder in a_n (left) and disorder in ω_n^2 (right) versus the strength of disorder ΔB. Each plotted mean escape time is the average of 1000 ensemble members. The ordinates are differently scaled. Although both kinds of disordered systems have equally distributed barrier energies B_n including the global equal mean barrier energy $B=4/3$, a complementary influence on the mean escape time occurs. Coupling parameter value: $\kappa=0.3$. Initial values: $p_n(t=0) \simeq 0.547$, $q_n(t=0)=0$.

yond the barrier. It is a relatively fast escape, because the mean escape time yields round about 5800 time units. In both simulations, breathers emerge. They tend to be situated at sites with lower barrier. Pinned breathers dominate the energy landscape more in the right than in the left simulation. One breather starting at site $n=30$ in case of disorder in a_n moves during the simulation time over ten sites to merge at $n=19$ with its neighboring breather inducing the escape. Such distinct mobility signature cannot be found in the right panel. There, the breather at $n=60$ exhausts little by little the energy of the ten nearest particles. Crucially, in both cases of disorder the starting breathers have too small amplitudes for an escape. They have to interact at least by an exchange of energy or, more effectively, they have to merge.

Since the chain needs due to the uniform initial conditions already disorder in the parameters (e.g., $\Delta B \neq 0$) to start interaction followed by any possible localization, the escape times for our system in case of $\Delta B \rightarrow 0$ could be rather long. For $\Delta B=0$ and uniform initial conditions, escape is impossible, because the initial particle energy is smaller than the barrier energy B and no interaction between the particles

occurs. Hence, the escape times for disorder in ω_n^2 could exhibit a minimum. Therefore, we calculate escape times also for exiguous ΔB. The results for the mean escape time are shown in Fig. 4 over a logarithmical ΔB axis for disorder in a_n (dark) and disorder in ω_n^2 (bright). The coupling strength and the initial momenta are the same as in Fig. 2. Indeed we find for disorder in ω_n^2 the shortest mean escape times for $\Delta B \approx 0.01$. Huge protractions for less disorder are not visible. On the other hand, when starting from nonflat initial states the problem of escape divergence for $\Delta B=0$ could be avoided. However, such a study is not in the scope of the present paper.

B. Influence of inhomogeneous barriers on the escape times

Let us again have a view on the on-site potentials and their barriers

$$U_n(q_n) = \frac{\omega_n^2}{2}q_n^2 - \frac{a_n}{3}q_n^3, \quad B_n = \frac{(\omega_n^2)^3}{6a_n^2}.$$

Disorder in a_n or in ω_n^2 is connected with inhomogeneous barriers and also with qualitatively different localization be-
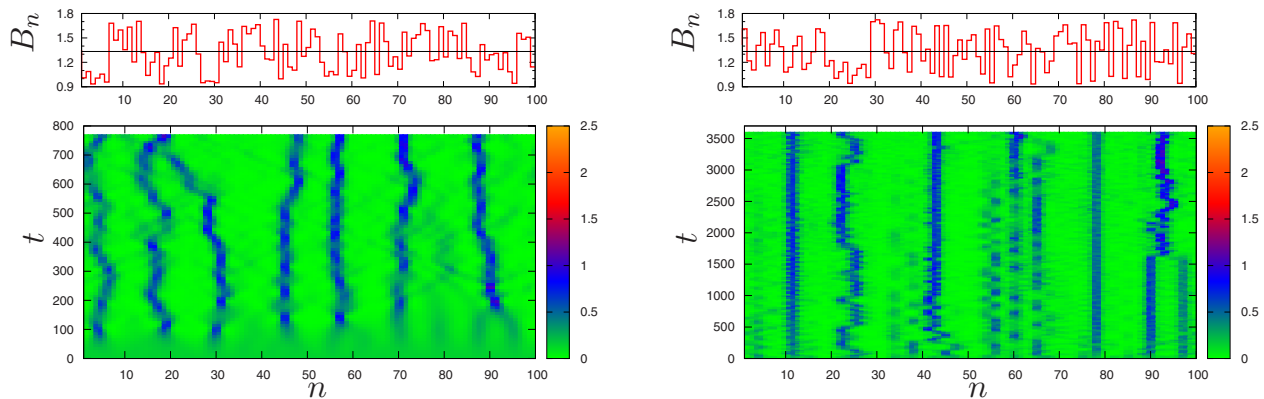
FIG. 3. (Color online) Density plots of $E_n(t)$ [Eq. (16)] for $\Delta B=0.4$. Left (right): disorder in a_n (ω_n^2), $n=19$ ($n=60$) is the first escaping particle. Coupling parameter value: $\kappa=0.3$. Initial values: $p_n(t=0) \simeq 0.547$, $q_n(t=0)=0$. The time-axis (ordinate) is differently scaled left against right. The breathers in the left seem to be less pinned or less numerously pinned. In both cases the initial visible breathers (dark traces) are not able to induce an escape. Only after clear visible interactions of more than one breather, an escape occurs. Above: the concrete randomized barrier energies B_n for each site n. The breathers tend to be situated at sites with low B_n, ergo at soft sites.
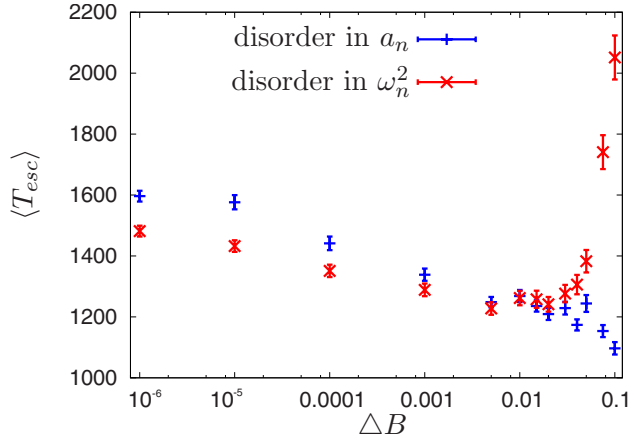
FIG. 4. (Color online) Mean escape times $\langle T_{esc} \rangle$ for disorder in a_n (dark) and disorder in ω_n^2 (bright) for small ΔB. Besides the logarithmical x axis the plots are made in an analogous manner to Fig. 2 including same parameters and initial conditions. For exiguous disorder it takes longer time until breathers grow, inducing the escape dynamics. Disorder in a_n produces for exiguous disorder strengths the slower escape times in contrast to larger disorder seen in Fig. 2.

FIG. 5. Mean escape times $\langle T_{esc} \rangle$ for disorder with constant B_n versus the disorder parameter ΔB. It is an analogous plot to Fig. 2, which shows the mean escape times for disorder in a_n and disorder in ω_n^2, respectively. Coupling parameter value: $\kappa = 0.3$. Initial values: $p_n(t=0) \simeq 0.547$, $q_n(t=0) = 0$. Inset: same data forming nearly a line with a logarithmical ordinate. This disorder with a strong disordered linear regime like disorder in ω_n^2 but homogeneous barriers B_n produces significantly longer mean escape times for $\Delta B > 0.25$.

havior. We have incorporated these kinds of disorder based on equal distributions of the barrier energies. Strictly speaking, if there is a straight influence of inhomogeneous barriers on the escape times, we could not extract it comparing the results of disorder in a_n with disorder in ω_n^2 for a fixed ΔB. By the way, this has been the motive for investigating exactly these kinds of disorder. Thus, we demonstrate in the following that the different escape times shown in Fig. 2 in Sec. III A must have other reasons. To this end, we consider now indirectly the influence of inhomogeneous barriers.

A spatially periodic system with inhomogeneous barriers is impossible to create; moreover, periodicity and inhomogeneity are rather a contradiction. In other words, we cannot separate the influences of nonperiodicity and different barrier energies for the investigation of escape events and escape times. However, we can create systems with nonperiodicity and homogeneous barriers. In Sec. II, we have already introduced the disorder with constant $B_n = B \equiv 4/3$ but variable a_n and ω_n^2. Due to the variable ω_n^2, the disorder with constant B_n and disorder in ω_n^2 have a similar strong effect on the linear regime. The escape times for disorder with constant B_n are plotted in Fig. 5. The coupling parameter is again $\kappa = 0.3$, and the initial conditions are $q_n(t=0) = 0$ and $p_n(t=0) \simeq 0.547$. Compared to disorder in ω_n^2, significantly longer mean escape times occur for $\Delta B > 0.25$—e.g., for $\Delta B = 0.4$ nearly double as long. The inset of Fig. 5 depicts the same data with a logarithmical y axis. Clearly, in the presented range, the mean escape time depends nearly exponentially on the disorder parameter in case of disorder with constant B_n. Most importantly, we infer that the inhomogeneous barriers facilitate the escape.

For the present study, a system size $N = 100$ was chosen because then the lattice system is large enough that wave phenomena such as spontaneous energy localization, breather formation, and their merging are supported and, on the other hand, the numerical computations are not too time

consuming. Furthermore, the results for the disordered system can be compared with the one obtained in Ref. [3] for the ordered chain of length $N = 100$. Nevertheless, simulations for the disordered system were performed also for larger chains (up to $N = 1000$ particles) yielding practically the same results.

IV. INFLUENCE OF DISORDER ON THE ENERGY LOCALIZATION

In the last sections, we have illustrated that starting from an initial flat state configuration, where each unit possesses by far less energy than the barrier height, pronounced energy localization is necessary to initiate an escape of the chain beyond the barrier. In fact, the initial energy distribution, given by

$$p_n(t=0) \simeq 0.547,$$

$$q_n(t=0) = 0 \Rightarrow E_n(t=0) \simeq 0.15 = 11.25\%B, \quad (17)$$

is homogeneous, i.e., it is a completely delocalized state, where each unit possesses an equal amount of energy. Due to the interaction between the units formation of breathers may ensue. The escape occurs when one breather concentrates sufficient energy on a *few* particles of the chain. Thus, these particles develop a critical configuration bringing one particle—the first escaping particle—sufficiently far beyond the barrier.

The required critical configuration may concern only a few particles while the rest of the chain may even stay less excited. In the numerical simulations, one rather observes the emergence of a pattern of breathers in the simulations. Measurements of energy localization could have problems to discern between patterns, which permit fast escapes or cause slow or hamper escapes. Therefore, the probable best mea-

surement is the mean escape time itself as the answer of the question, how fast does the chain localize the energy reaching the critical configuration for an escape? Investigations in the last section show that for not too small values of the disorder parameter ΔB disorder in ω_n^2 reduces and disorder in a_n expedites the process of developing such energy localization which permits an escape.

In the following, the intention is to gain more insight into the impact of disorder on the process of energy localization. The energy localization is rather a physical feature, which does not lead strictly to a certain physical quantity. Nonetheless any measurement of energy localization should detect our initial state as a perfectly delocalized state. In the following section, we investigate time-continuous energy localization quantities based on the site energies $E_n(t)$ defined in Eq. (16). First, we investigate the partition number. Second, we consider the time-evolution of the vertices of the energy relief.

A. Partition number

The partition number for a system with N particles is defined by

$$P(t) = \frac{\left(\sum\limits_{n=1}^{N} E_n\right)^2}{\sum\limits_{n=1}^{N} E_n^2} = \frac{E^2}{\sum\limits_{n=1}^{N} E_n^2}. \qquad (18)$$

Due to the conservation of energy, $P(t)$ is the reciprocal of the quadratic mean of the N particle energies E_n. Hence, the co-domain of the partition number lies in the interval $1 \leq P(t) \leq N$. A totally localized energy on one particle leads to $P=1$, whereas a completely homogeneous distribution (for example, our initial state) yields $P=N$. One could say $P(t)$ measures the number of the strongly excited sites [4].

For a reasonable statistical analysis, we consider the dynamics for the different realizations of disorder up to the point, when the chain is in the process of escaping or has already realized the escape. The prerequisite to escape is connected with sufficiently pronounced degree of localization and the emergence of energy localization in the form of breathers which is accomplished when one or a few particles are pushed behind the barrier exceeding the position $q_n > 3\omega_n^2/(2a_n)$. Thus, we terminate each simulation, when the first particle has reached a negative on-site potential energy, respectively, the second zero-point

$$U_n(q_n) < 0 \Leftrightarrow q_n > \frac{3}{2}\frac{\omega_n^2}{a_n}. \qquad (19)$$

The number of ensemble members

$M(t) :=$ number of chains for which inequality

$\qquad$ (19) was never true until the time $t \qquad$ (20)

decreases with the time and hence, the mean partition number is given by

$$\langle P \rangle_{M(t)} = \frac{1}{M(t)}\sum_{m=1}^{M(t)} P_m(t). \qquad (21)$$

With the subscript $M(t)$, we denote this version of ensemble average also for other quantities.

Figure 6 displays mean partition numbers for the kinds of disorder in a_n (left), in ω_n^2 (right) and for linear disorder (inset of the upper right panel). $M(t)$ starting from $M(t=0)=1000$ is plotted in the panels below.

Dashed curves belong to $\Delta B=0.15$, for which the mean escape time $\langle T_{esc} \rangle$ in case of disorder in ω_n^2 is three times larger than for disorder in a_n. Solid curves represent the value $\Delta B=0.4$ for which escape of chains evolving with disorder in ω_n^2 is nearly ten times slower than their counterpart with disorder in a_n. Depicting also one nearly ordered nonlinear case, the quantities (dashed-dotted curves) for $\Delta B=0.001$ in case of disorder in a_n are shown.

The stronger energy localization is, the lower is the associated partition number. A few effects causing the energy localization can be indirectly elicited: first, more disorder speeds up the beginning of energy localization. Comparing linear disorder with nonlinear disorder for exiguous disorder $\Delta B=0.001$, we second infer that nonlinearity causes a strong energy localization. Third, a certain energy localization ($\langle P \rangle_{M(t)} \approx 50$—inset in the upper right panel)—appears even in systems with significant disorder without nonlinearity. Fourth, by means of the solid curves for the ensembles evolving with large disorder $\Delta B=0.4$, we see that disorder in a_n beats the partition number conspicuously more than disorder in ω_n^2, which is in accordance with shorter escape times for disorder in a_n. We interpret this behavior as a consequence of Anderson localization impeding the mobility of the breathers in case of disorder in ω_n^2. Thus, in that case, collisions along with merging of breathers occur less numerously.

Disorder in a_n: the partition number strongly drops after approximately 300 time steps detecting arising breathers. After the first local minimum, the typical *breathing* of the breathers is reflected by the graph of the partition number. After half of the 1000 chains has escaped—at $t \approx 1250$, $\langle P \rangle_{M(t)}$ saturates at a value of approximately 25. For higher ΔB, the energy localization occurs faster and the breathing is less pronounced. Since all curves nearly saturate at a similar level, we depict the differences with reference lines, which have a distance of 2.5 to each other. It is interesting that in case of strong disorder $\Delta B=0.4$ in a_n, the energy localization stops at about 28 above the curves for $\Delta B=0.15$ and $\Delta B=0.001$, although the mean escape time is much shorter. Since for $\Delta B=0.4$ very low barriers can be found in the lattice, the chain needs less localization than for a lower ΔB. Whether or not increasing disorder in a_n assists energy localization, the question would stay unanswered. But as we have discussed in Sec. II, the disorder in the nonlinearity with homogeneous harmonicity parameters belong inseparably to inhomogeneous barriers.

The partition numbers in case of disorder in ω_n^2 (right) saturate before most of the chains have escaped contrary to the behavior for disorder in a_n. The Anderson localization as
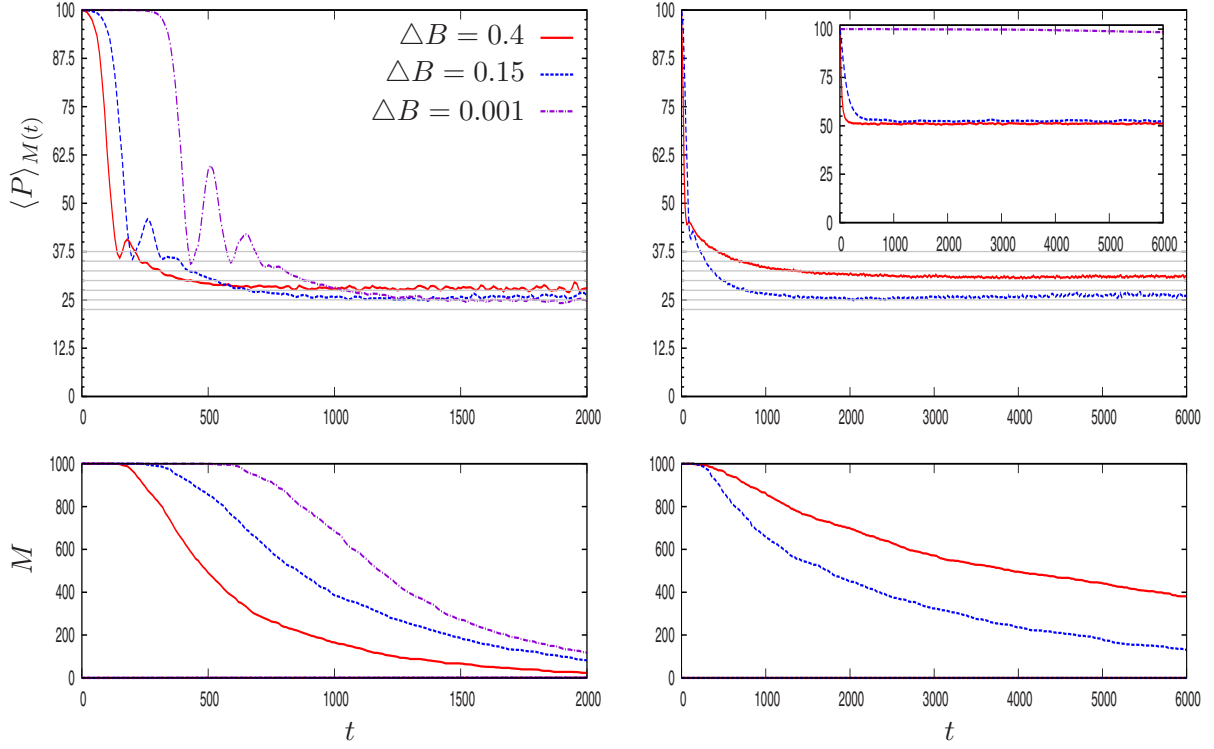
FIG. 6. (Color online) Mean partition number $\langle P \rangle_{M(t)}$ in the above panels and the number of in the well remaining chains $M(t)$ [Eq. (20)] in the bottom panels versus time for disorder in a_n in the left panels, disorder in ω_n^2 in the right panels. In the inset $\langle P \rangle_{M(t)}$ for linear disorder is depicted. Selected values of the disorder parameter: $\Delta B = 0.001$ (dashed-dotted), 0.15 (dashed), and 0.4 (solid). $M(t=0)=1000$ chains are pursued. Coupling parameter value: $\kappa = 0.3$. Initial values: $p_n(t=0) \simeq 0.547$, $q_n(t=0)=0$.

a hindrance for moving breathers in case of linear disorder in ω_n^2 could explain on the one hand the long escape times and on the other hand the little differences of the energy localization, because Anderson localization itself decreases the partition number. In the following, we concentrate directly on energetically highest vertices of the $E_n(t)$.

B. Vertices of the energy relief

Since one particle sufficiently far behind the barrier is able to pull the rest of the chain, an interesting quantity represents the evolution of the highest relative particle energy of the chain given by

$$\delta E_{1\text{st max}}(t) := \frac{1}{E} \max_{n=1}^{N} E_n(t).$$

It measures the capability of the respective disordered system to localize a huge part of the energy on one site more concretely than the partition number. Our initial value $p_n(0) \simeq 0.547$ yields $\delta E_{1\text{st max}}(0)=1\%$.

Furthermore, we also compute the second highest particle energy by taking the maximum of the sequence E_n without the first highest value—and compute analogously the third highest value and so on. We denote this procedure with " $*$ " and the ith highest particle energy is given by

$$\delta E_{i\text{th max}} := \frac{1}{E} \overset{*}{\max} E_n(t). \tag{22}$$

As discussed in the last sections, we are interested in different ensembles of systems distinguished by the kind and the strength of disorder. Hence, we calculate the ensemble average $\langle \delta E_{i\text{th max}} \rangle_{M(t)}$ over $M(t=0)=1000$ simulations as described in the last section [see expressions (19)–(21)]. The respective ten mean highest relative particle energies in case of disorder in ω_n^2 (right panel) and a_n (left panel) are shown in Fig. 7 for $\Delta B = 0.4$.

We have obtained faster escapes together with lower partition numbers for $\Delta B = 0.4$ in case of disorder in a_n compared to disorder in ω_n^2 (cf. Secs. III A and IV A). Except for the beginning, we observe here faster and stronger energy localization for disorder in a_n. At $t \approx 700$ the curves for disorder in a_n saturate, i.e., they fluctuate around fixed values. The fluctuations result from the diminishing number of ensemble members $M(t)$ due to the short escape times. The energy localization does not continue to increase, because the chains with most localized energy achieve escape and hence they leave the ensemble. The curves for disorder in ω_n^2 saturate at $t \approx 2000$ (we have also observed later times). For less disorder, we find that the level of saturation is higher, since in that case, due to less differing barrier heights, the chain has to target higher energy vertices for an escape.

Since in the exemplary energy landscape $E_n(t)$ shown in Fig. 3 single site breathers and also multibreathers were visible, multiple $\delta E_{i\text{th max}}$ could lead to only one multibreather.
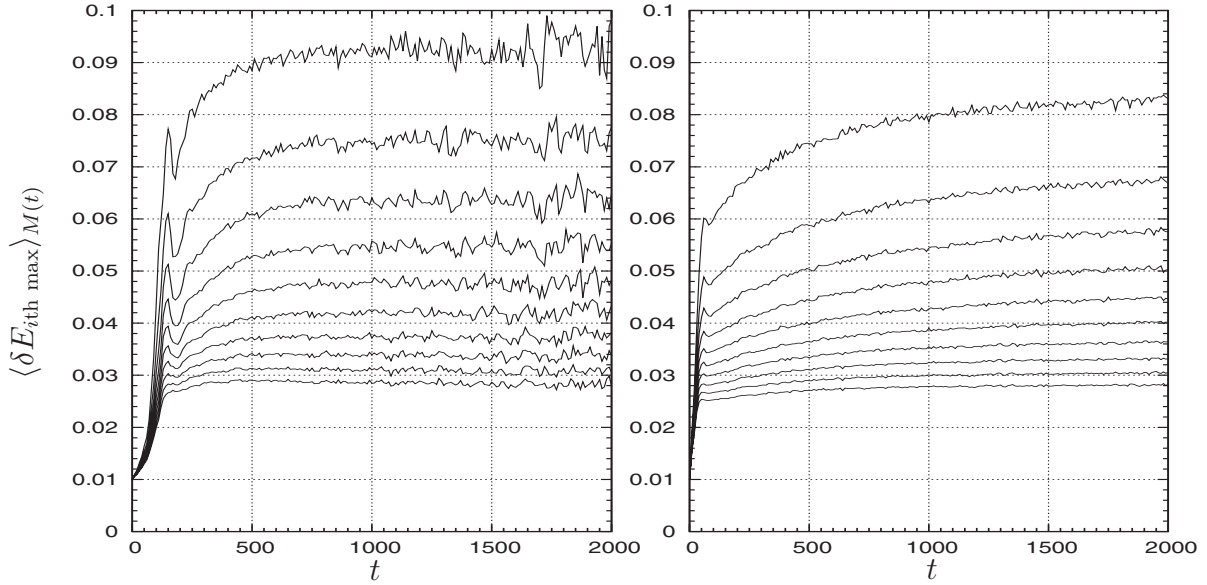
FIG. 7. The 10 mean highest relative particle energies $\langle \delta E_{i\text{th max}} \rangle_{M(t)}$ [Eq. (22)] versus time for disorder in a_n (left) and disorder in ω_n^2 (right). Parameter value: $\Delta B = 0.4$. Coupling parameter value: $\kappa = 0.3$. Initial values: $p_n(t=0) \simeq 0.547$, $q_n(t=0) = 0$. At the beginning, the ensemble has $M(0) = 1000$ members. Since $M(t)$ decreases with time, the curves especially for disorder in a_n with the faster escape dynamics fluctuate strongly at the end. At the beginning, the fluctuations are caused by similar collective breathing. Then, especially the highest curves for disorder in a_n increase faster and outperform those for disorder in ω_n^2. For an escape, the highest vertices are important and thus escapes occur at longer times for disorder in ω_n^2.

Thus, the mean highest relative particle energies are not suited to measure the number of breathers in the lattice. Therefore, we introduce a simple counter for the vertices of the energy relief

$$Z_g(t) = \sum_{\{n | E_n \rangle E_{n-2}, E_{n-1}, E_{n+1}, E_{n+2} \wedge E_n \rangle g(E/N)\}} 1, \qquad (23)$$

which is proposed to count vertices, which have a distance of at least three sites to each other. The subscript g is connected with an additional condition for counting, which offers information about lower and higher vertices. E/N is the (constant) average of the E_n over the N particles. We have performed calculations for $g = 1$, 3, 5, and 7. Figure 8 depicts the corresponding mean values for $\Delta B = 0.4$. The mean number of vertices higher than E/N ($g = 1$—solid curve) drops slower for disorder in ω_n^2. The breathers encounter difficulties accumulating energy from the lattice, which is somehow stored in localized Anderson modes. One finds also more vertices with $E_n > 3E/N$ (dashed curves) for disorder in ω_n^2, but disorder in a_n generates more high energy vertices, especially those with $E_n > 7E/N$ (dotted curves). We have performed these simulations also for $\Delta B = 0.15$. The differences between disorder in a_n and disorder in ω_n^2 are less significant but qualitatively the same as for $\Delta B = 0.4$.

We have noted earlier that without disorder, typically low-amplitude breathers can move through the lattice, forming high vertices as a result of breather merging in the energy relief. Disorder in ω_n^2 seems to disable such a spatial freedom, particularly for low-energy vertices exhibited in the disordered linear regime. But the building of a quite craggy energy relief is still intact. Probably nearly all vertices are pinned. Thus, for disorder in ω_n^2, the formation of large-amplitude breathers occurs not so often as for disorder in a_n, for which the periodic linear regime prohibits Anderson modes and mobile breathers often merge.

We have also investigated the mean number of vertices with the less strict condition $E_n > E_{n-1}, E_{n+1}$ and find only for $g = 1$ significantly more vertices. Hence, the distance of two neighboring breathers is usually more than two lattice sites. Furthermore, we infer that the plots of the mean highest relative particle energies mostly entail vertices of different breathers. Broad multibreathers were not seen in our simulations.

Next, we investigate whether the vertices have a tendency to occur at specific sites, which is important bearing in mind the inhomogeneity of the barriers.

V. MOST AND LEAST PREFERRED ON-SITE POTENTIALS

In Sec. III B, we have investigated the influence of inhomogeneous barriers on the escape times. The longest mean escape times have been found for disordered systems with constant barrier energies B_n. We have inferred that inhomogeneous barriers are a feature which facilitates the escape giving one quite clear reason for the faster escapes times in case of disorder in a_n compared to the ordered limiting case. For variable ω_n^2, the escape times increase with more degree of disorder due to the disordered linear regime, whereby a trend to pinned, nonmerging breathers is seen. Moving breathers are not only able to merge with each other. They can also search low barriers, where their energy suffices to push one particle beyond the barrier. We think that this scenario dominates the escapes dynamics in the case of disorder
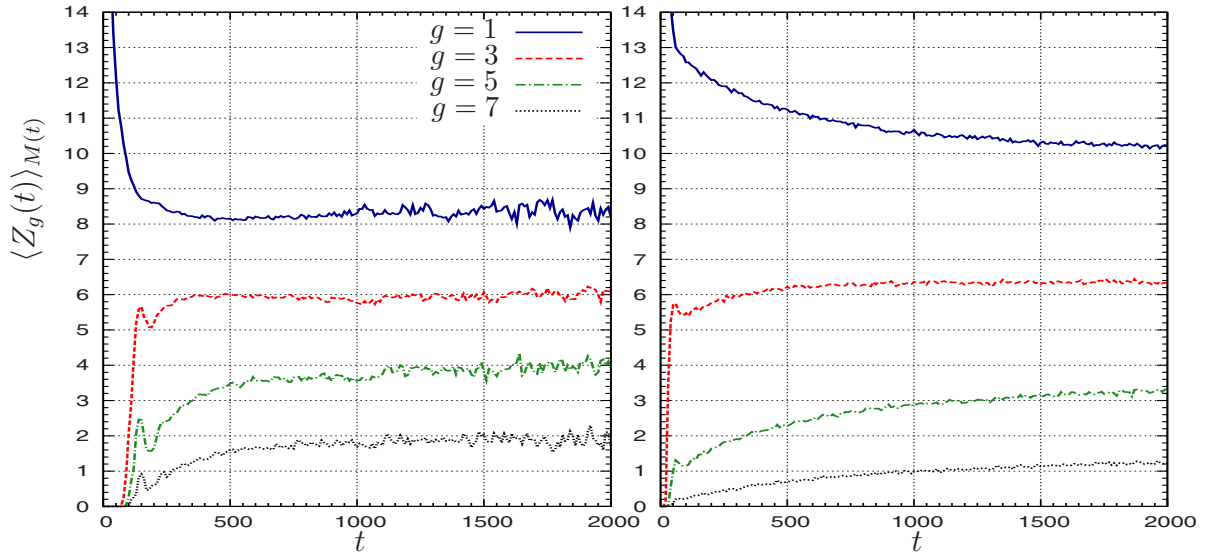
FIG. 8. (Color online) Mean number of vertices $\langle Z_g(t) \rangle_{M(t)}$ [Eq. (23)] of the energy relief $E_n(t)$ versus time for disorder in a_n (left) and disorder in ω_n^2 (right). Parameter value: $\Delta B = 0.4$. Coupling parameter value: $\kappa = 0.3$. Initial values: $p_n(t=0) \simeq 0.547$, $q_n(t=0)=0$. At the beginning the ensemble has $M(0)=1000$ members. With g, we distinguish the energy height of the vertices. Only vertices that are more than g times higher than the mean particle energy are counted. For allocation of the line types, see key. For disorder in ω_n^2, one finds more small-amplitude localized oscillations, but disorder in a_n leads to more large-amplitude breathers ($g=7$). Hence, we can imagine a more cliffy relief with less immense crests than for disorder in a_n. This type of energy relief complicates the escape.

in a_n. An additional advantage is given, if from the beginning of the localization of energy, sites with lower barriers would be more preferred than those with higher barriers.

We calculate for $t > 0$ the most and least preferred sites with their barrier energies given as follows:

$$b_{\text{most}} = B_m | \{ E_m = \max_{n=1}^{N}(E_n) \},$$

$$b_{\text{least}} = B_l | \{ E_l = \min_{n=1}^{N}(E_n) \}. \qquad (24)$$

The actual location is not of interest. In Fig. 9, we plot the temporal behavior of the ensemble average (as introduced in Sec. IV A) for the disorder parameter $\Delta B = 0.4$.

The reference line shows the mean barrier energy at $B = 4/3$. The range of the ordinate is bounded from the maximal possible barrier energy $B + \Delta B$ and the minimal possible one $B - \Delta B$. At the beginning, $\langle b_{\text{most}} \rangle_{M(t)}$ drops nearly instantaneously to one of the lowest thinkable barrier energies— maybe it is the lowest. In contrast, $\langle b_{\text{least}} \rangle_{M(t)}$ rockets up. We suppose that this phenomenon appears on the complete lattice, i.e., the energy drops instantaneously into the rather soft local potentials with lower barriers.

We know from the last sections that after approximately $t = 500$ time units, a pronounced energy localization has occurred. At this time, the curves in Fig. 9 begin to fluctuate around fixed values. For both kinds of disorder lattice sites with on-site potentials with low barriers are preferred to be distributed with energy, which facilitates the escape. The (dashed) $\langle b_{\text{most}} \rangle_{M(t)}$ for disorder in ω_n^2 is under the (solid) $\langle b_{\text{most}} \rangle_{M(t)}$ for disorder in a_n situated. The preference of the energy to remain at soft sites is more dominant for disorder

in ω_n^2 than for disorder in a_n, for which nonetheless faster escapes are observed. An explanation is the larger mobility in case of disorder in a_n. By moving through the lattice, the breather visits a number of sites increasing $\langle b_{\text{most}} \rangle_{M(t)}$. From the curves for $\langle b_{\text{least}} \rangle_{M(t)}$, it follows that breathers avoid sites with higher barriers, which could appear as barricades for moving breathers especially in case of disorder in ω_n^2.

In the exemplary simulations presented in Sec. II (see Fig. 3), the breathers evolve mostly in valleys of the relief of barrier energies. Long escape times occur probably in lattices, where these barricades are unfavorably situated hindering the merging of breathers. Contrarily, one might ask how a lattice, defined by the sequence of barriers B_n and the kind of disorder, should be constructed to accomplish a fast escape? First, it should have kind of pores, i.e., sites with very low barriers. Second, a low number of barricade sites with large barriers is advisable. Third, if the breathers tend to move to low barriers, a relief of weak slopes with the pore or pores at its lowest point(s) would expedite additionally an escape. And of course, one should "choose" to use only a variable nonlinearity parameter to make the barrier inhomogeneous.

VI. SUMMARY

We have investigated the deterministic and conservative dynamics of a one-dimensional chain of N harmonically coupled particles. Each particle evolves in an individual cubic on-site potential, which exhibits a barrier separating a metastable state from an attractive domain. The shape of the cubic potential is characterized by a harmonicity parameter and an anharmonicity parameter. Our main interest has been directed to the influence of two different kinds of parametric
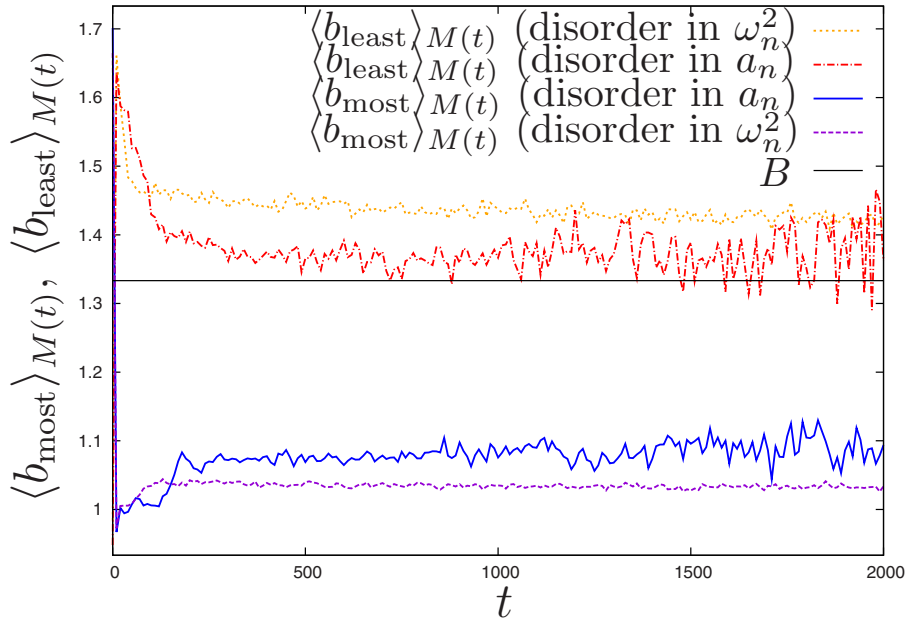
FIG. 9. (Color online) Mean values of the barrier energy of the most and least preferred sites $\langle b_{most}\rangle_{M(t)}$ and $\langle b_{least}\rangle_{M(t)}$ for $t > 0$. Parameter value: $\Delta B = 0.4$. Coupling parameter value: $\kappa = 0.3$. Initial values: $p_n(t=0) \simeq 0.547$, $q_n(t=0) = 0$. The simulations are made with $M(t=0) = 1000$ chains and for disorder in ω_n^2 and disorder in a_n (see key). The reference line shows the mean barrier energy at $B = 4/3$. In the first few time steps, the on-site potential with one of the lowest barrier is energized and the potential with one of the higher barrier de-energized mostly. Later, one finds plateaus, which evidence that softer sites with lower barrier are more preferred—especially in case of disorder in ω_n^2, wherein the breathers tend to be pinned at these sites.

disorder on the system behavior, especially the escape dynamics. Disorder is involved either in the harmonicity or anharmonicity parameter of the on-site potentials yielding a uniform distribution of the barrier heights around a mean barrier energy. A measurement of the strength of disorder has been introduced, allowing a comparison between the behavior of the systems with different kinds of disorder.

Initially, the chain is situated at the bottom of the potential wells and all of its units possess equal momenta, which is the starting configuration is a flat state. Crucially, the energy content of each unit does not suffice for immediate barrier crossing. Ensuing interaction between the units of the chain may lead to breather formation going along with such pronounced energy localization that the chain passes through the transition state with subsequent escape over the barrier. Interestingly, with increasing strengths of disorder, the mean escape time decreases for disorder in the anharmonicity parameter and increases for disorder in the harmonicity parameter. Typically one observes a scenario of rather movable breathers for disorder in the anharmonicity parameter and in contrast a picture of pinned breathers for disorder in the harmonicity parameter hindering the merging to form large-amplitude breathers. We have confirmed that the reason for this difference is indeed related to the Anderson localization present in the linear limiting periodic case of the latter system.

Furthermore, we have considered a third kind of disorder for which both the harmonicity as well as anharmonicity parameter are taken as random quantities being arranged in such a way that the resulting barrier energies are all equal along the chain. Strikingly, for this kind of disorder, there results longer mean escape times than in the case of disorder in the harmonicity parameter, for which the barrier heights are inhomogeneous. Conclusively, inhomogeneous barrier heights facilitate faster escape.

We also have pursued the question that on-site potentials are mostly preferred or avoided when the energy is distributed among the lattice units. For disorder either in the harmonicity parameter or anharmonicity parameter, the particle with the largest energy evolves on average in a softer local potential, which has per construction a lower barrier. It seems that the arising breathers do not only prefer to be centered localized at soft local potentials, but they are also generated rather at these sites. The site most avoided by the energy distribution has on average a barrier height higher than the mean barrier energy. Obviously sites with large barriers act as barricades for breathers moving through the lattice—foremost in case of disorder in the harmonicity parameter.

Finally, the presented analysis of different kinds of disorder, having purposeful differences and similarities, could help generally to better understand phenomena of disordered, nonlinear lattices particularly with view to the formation process of discrete breathers.

[1] H. Risken, *The Fokker-Planck Equation* (Springer-Verlag, New York, 1989).

[2] P. Hänggi, P. Talkner, and M. Borkovec, Rev. Mod. Phys. **62**, 251 (1990).

[3] D. Hennig, S. Fugmann, L. Schimansky-Geier, and P. Hänggi, Phys. Rev. E **76**, 041110 (2007).

[4] S. Flach and C. R. Wilis, Phys. Rep. **295**, 181 (1998).

[5] S. Flach and A. Gorbach, Phys. Rep. **467**, 1 (2008).

[6] D. L. Shepelyansky, Phys. Rev. Lett. **70**, 1787 (1993).

[7] M. I. Molina, Phys. Rev. B **58**, 12547 (1998).

[8] G. Kopidakis, S. Komineas, S. Flach, and S. Aubry, Phys. Rev. Lett. **100**, 084103 (2008).

[9] A. S. Pikovsky and D. L. Shepelyansky, Phys. Rev. Lett. **100**, 094101 (2008).

[10] I. García-Mata and D. L. Shepelyansky, Phys. Rev. E **79**, 026205 (2009).

[11] S. Flach, D. O. Krimer, and Ch. Skokos, Phys. Rev. Lett. **102**, 024101 (2009).

[12] M. Johansson, G. Kopidakis, S. Lepri, and S. Aubry, EPL **86**, 10009 (2009).

[13] D. Hennig, L. Schimansky-Geier, and P. Hänggi, EPL **78**, 20002 (2007).

[14] S. Fugmann, D. Hennig, L. Schimansky-Geier, and P. Hänggi, Phys. Rev. E **77**, 061135 (2008).

[15] D. Hennig, S. Fugmann, L. Schimansky-Geier, and P. Hänggi, Acta Phys. Pol. B **39**, 1125 (2008).

[16] S. Fugmann, D. Hennig, S. Martens, and L. Schimansky-Geier, Physica D **237**, 3179 (2008).

[17] G. Kopidakis and S. Aubry, Physica D **130**, 155 (1999).

[18] S. S. Albuquerque, F. A. B. F. de Moura, and M. L. Lyra, Physica A **357**, 165 (2005).

[19] H. Shima, S. Nishino, and T. Nakayama, J. Phys.: Conf. Ser. **92**, 012156 (2007).

[20] R. Reigada, A. H. Romero, A. Sarmiento, and K. Lindenberg, J. Chem. Phys. **111**, 1373 (1999).